



THE UNIVERSITY *of* EDINBURGH

## Edinburgh Research Explorer

# Liquid crystal multi-mode lenses and axicons based on electronic phase shift control

### Citation for published version:

Kirby, AK, Hands, PJW & Love, GD 2007, 'Liquid crystal multi-mode lenses and axicons based on electronic phase shift control' *Optics Express*, vol 15, no. 21, pp. 13496-13501. DOI: 10.1364/OE.15.013496

### Digital Object Identifier (DOI):

[10.1364/OE.15.013496](https://doi.org/10.1364/OE.15.013496)

### Link:

[Link to publication record in Edinburgh Research Explorer](#)

### Document Version:

Publisher's PDF, also known as Version of record

### Published In:

*Optics Express*

### Publisher Rights Statement:

This paper was published in *Optics Express* and is made available as an electronic reprint with the permission of OSA. The paper can be found at the following URL on the OSA website: [<http://dx.doi.org/10.1364/OE.15.013496>]. Systematic or multiple reproduction or distribution to multiple locations via electronic or other means is prohibited and is subject to penalties under law.

### General rights

Copyright for the publications made accessible via the Edinburgh Research Explorer is retained by the author(s) and / or other copyright owners and it is a condition of accessing these publications that users recognise and abide by the legal requirements associated with these rights.

### Take down policy

The University of Edinburgh has made every reasonable effort to ensure that Edinburgh Research Explorer content complies with UK legislation. If you believe that the public display of this file breaches copyright please contact [openaccess@ed.ac.uk](mailto:openaccess@ed.ac.uk) providing details, and we will remove access to the work immediately and investigate your claim.



# Liquid crystal multi-mode lenses and axicons based on electronic phase shift control

Andrew K. Kirby, Philip J. W. Hands, and Gordon D. Love

Durham University, Dept. of Physics, Durham, DH1 3LE, UK

**Abstract:** We report on the principle of operation, construction and testing of a liquid crystal lens which is controlled by distributing voltages across the control electrodes, which are in turn controlled by adjusting the phase of the applied voltages. As well as (positive and negative) defocus, then lenses can be used to control tip/tilt, astigmatism, and to create variable axicons.

©2007 Optical Society of America

OCIS codes: (230.0230) Optical Devices; (230.3720) Optical Devices; liquid crystal Devices.

---

## References and links

1. S. Kuiper and H. H. W. Hendricks, "Variable-focus liquid lens for miniature cameras," *Appl. Phys. Lett.* **85**:1128-1130 (2004).
  2. Varioptic Company ([www.varioptic.com](http://www.varioptic.com))
  3. A. Kaplan, N. Friedman, and N. Davidson, "Acousto-optic lens with very fast scanning," *Opt. Lett.* **26**:1078-1080 (2001).
  4. D. Y. Zhang, N. Justis, and Y. H. Lo. "Integrated fluidic adaptive zoom lens," *Opt. Lett.* **29**, 2855-2857 (2004).
  5. L. Dong, A. K. Agarwal, D. J. Beebe and H. Jiang, "Adaptive liquid microlenses activated by stimuli responsive hydrogels," *Nature* **442**, 551-554 (2006).
  6. L. G. Commander, S. E. Day, and D. R. Selviah, "Variable focal length microlenses," *Opt. Commun.* **177**, 157-170 (2000).
  7. A. F. Naumov, M. Yu. Loktev, I. R. Guralnik, and G. Vdovin, "Liquid crystal adaptive lens with modal control," *Opt. Lett.* **23**, 992-994 (1998).
  8. A. F. Naumov, G. D. Love, M. Yu. Loktev and F. L. Vladimirov, "Control optimization of spherical modal liquid crystal lenses," *Opt. Express* **4**, 344-352 (1999).
  9. O. A. Zayakin, M. Yu. Loktev, G. D. Love, and A. F. Naumov, "Cylindrical adaptive lenses," *Proc. SPIE* **3983**, 112-117 (1999).
  10. A. K. Kirby and G. D. Love, "Fast, large and controllable phase modulation using dual frequency liquid crystals," *Opt. Express* **12**, 1470-1475 (2004).
  11. G. Love, J. Major, and A. Purvis, "Liquid crystal prisms for tip—tilt adaptive optics," *Opt. Lett.* **19**, 1170-1172 (1994).
  12. P. J. W. Hands, S. A. Tatarkova, A. K. Kirby, and G. D. Love, "Modal liquid crystal devices in optical tweezing: 3D control and oscillating potential wells," *Opt. Express* **14**, 4525-4537 (2006).
- 

## 1. Introduction

Considerable work has been carried out in the field of electronically variable lenses, and a variety of approaches have been described, including electro-wetting [1, 2], acousto-optics [3] and fluid-filled lenses [4, 5]. There is also considerable interest in liquid crystal (LC) lenses and again a variety of control techniques have been described – many of which are reviewed in Ref. [6]. One particular method, which we have reported previously, of controlling LC lenses is known as *modal control* [7, 8]. Here a very high resistance electrode is used so that a simple LC cell behaves, electrically, in a similar way to a transmission line. The result is that a voltage profile, and hence phase profile, can be distributed across an LC cell without the use of pixels or multiple electrodes.

Despite its simplicity, a practical problem associated with building LC lenses is the difficulty of fabricating an extremely thin layer of Indium Tin Oxide needed for the very high resistance electrode ( $\sim 5\text{M}\Omega/\text{sq}$ ). Producing the required thickness with good uniformity is problematic, and the deposition process typically has a low yield. Different lenses will have slightly different electrode resistances and this, coupled with the fact that modal control is also

very dependent on the precise cell thickness, means that each individual lens needs to be calibrated separately. Also, the minimum diameter of a modal lens is limited to about 2mm – below this size the required resistivity of the ITO layer exceeds some  $10\text{M}\Omega/\text{sq}$ . Finally modal LC lenses must always be either positive or negative. It is not possible to switch between a diverging and converging lens.

Here we present a different approach to distributing a voltage across an LC cell, that avoids limitations described above, which uses only medium resistance ITO coatings – which are commercially widely available. The method is based on the control of the phase of the driving electrical signals at each end of the cell. The voltage distribution is also not so critically dependant on the cell parameters (because it is easier to obtain medium resistance ITO coatings and the voltage profile does not depend on the cell thickness and capacitance) – and thus they are easier to calibrate. Finally they may be used to create a variety of phase profiles – not only defocus. This method of using phase control was proposed in Ref [9], and in this paper we describe the operation fully and give a range of experimental results.

## 2. Device structure and operation

The basic structure of the device is illustrated in Fig. 1. It is a conventional LC cell aligned for phase modulation – with the rectangular substrates arranged orthogonally or so that electrical contacts can be made to both ends of each substrate.

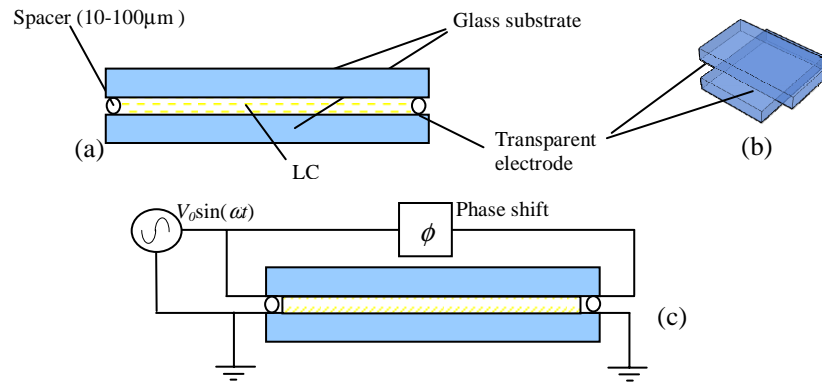


Fig. 1. 1-D schematic of LC device construction and of the electrode configuration used to produce a cylindrical lens. The same AC voltage is applied to each end of the cell – but with a phase shift. (a) and (b) show the cell construction and (c) shows the electrical connections used to drive the cell. A conventional AC source is used along with a phase shifter (the symbols have their conventional meanings).

The device is essentially a conventional LC cell constructed from rectangular substrates which are arranged as shown, so that electrical contacts can be made to both sides of each substrate. The substrates also have the usual alignment and electrode coatings (not shown). The electrode resistance was  $\sim 5\text{-}10\text{ k}\Omega/\text{sq}$ . Anti-parallel alignment was used. The LC material was LC1001 (Niopik, Russia) which is a dual frequency LC – but any typical LC material used for phase applications would also be suitable. The cell was 10mm in length, but the minimum size is only limited only by the constructional practicalities.

The principle of operation is illustrated by the most basic one-dimensional configuration of a cylindrical lens, the schematic of which is shown in Fig. 1, and by Fig. 2, which shows the results of simulations of the voltage profiles. The phase profiles are calculated from separate experimental data of the phase versus the voltage. In this configuration, one substrate of the device is grounded (lower electrode, as shown in Fig. 1), and the two opposing sides of the upper electrode are driven by a sinusoidal AC voltage, with a phase shift,  $\phi$ , between them. When  $\phi$  is set to  $180^\circ$ , then the RMS voltage profile measured across the upper electrode, with respect to ground takes on a “V-profile” as illustrated by the solid

blue line in Fig. 2 ( $V_{\text{rms}}$  180deg), varying from  $6.33V_{\text{rms}}$  (for a driving voltage of  $18V_{\text{pp}}$ ) at the driven edges of the cell to  $0V_{\text{rms}}$  in the centre. The dashed blue line (optical 180deg) indicates the equivalent optical phase shift. The specifics of the phase profile will depend on the LC material used (here it is LC1001) but the general shape will be the same.

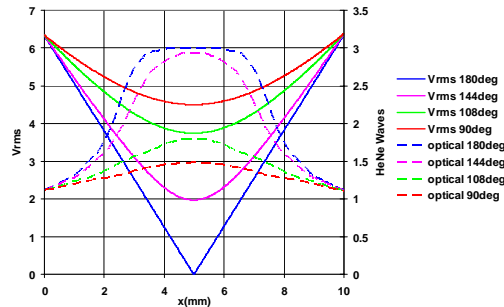


Fig. 2. Variation in phase (dashed) and RMS voltage (solid) profiles versus distance along an LC cell, for different values of the inter-electrode phase,  $\phi$ . Applied voltage,  $V_0=18V_{\text{pp}}$ . The cell (active area) length was 10mm.

It can be seen that in this configuration there is a plateau in the centre of the optical phase profile, because the voltage across the cell in that region drops below the threshold voltage of the LC. The plateau can be eliminated in one of two ways: i) by adjusting the phase between the opposing ends of the upper electrode and ii) by adding a constant bias voltage.

Figure 2 also shows the effect on the rms voltage and optical phase profiles with respect to variations in the inter-electrode phase shift,  $\phi$ . It can be seen that, as  $\phi$  is reduced, the voltage profile takes on a more curved shape and does not drop to  $0V_{\text{rms}}$  in the centre of the electrode, and that the plateau in the optical phase profile is therefore reduced.

Adding a bias voltage requires that a second driving voltage with  $\phi = 0^\circ$  be summed with that described above, as shown in Fig. 3. The effect of the bias voltage is to shift the voltage profile such that in no region of the device does the voltage drop below the threshold voltage of the LC. In theory, both techniques (adding a bias voltage or by adjusting the phase) work equally well, but from our practical experience the bias voltage method was easier to implement.

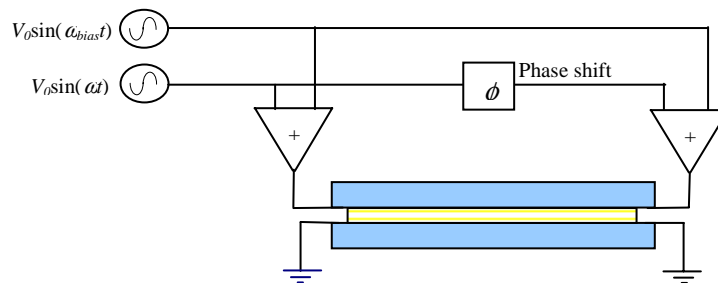


Fig. 3. Adding bias voltage to remove optical phase plateau (one dimensional case).

The description given above illustrates how a lens-like positive cylindrical lens profile can be generated. However the use of dual frequency LC materials allows the production of both positive and negative lens shapes. A dual frequency LC exhibits a low-frequency inversion of the sign of the dielectric anisotropy, such that an applied field with a frequency above the inversion frequency causes the LC director to realign with the plane of the cell, rather than normal to it – i.e. the LC can be driven ‘on’ by a low frequency field and ‘off’ by a high frequency field [9]. If both high and low frequency fields are applied simultaneously, the LC

responds essentially to the difference of the opposing torques, and settles at a corresponding equilibrium. In essence – a uniform low frequency field turns the whole LC cell on, and then a high frequency field, controlled by using phase shifts as described earlier, turns the areas of the cell closest to the edge off – therefore producing a negative lens.

Setting up a voltage profile as shown in Fig. 4, the differential ( $V_{LF}-V_{HF}$ ) takes on a form as shown, with a central peak, giving rise to a negative-lens shape as shown.

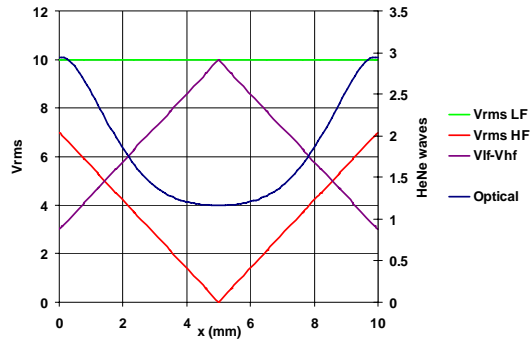


Fig. 4. Voltage and optical phase profiles used to produce a negative lens using dual frequency LC. A high frequency V- profile (red line) is generated, as described earlier. A low frequency constant bias voltage (green line) is also added to the cell. The LC responds to the difference of these voltages (purple line) and thus the phase profile of a negative lens (blue line) is produced.

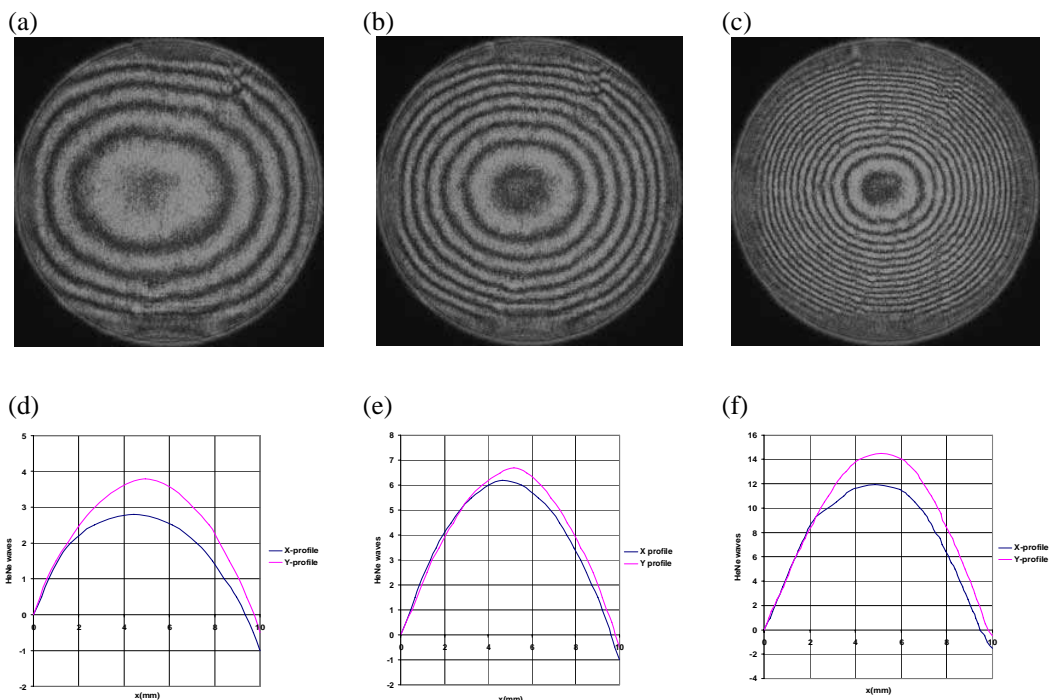


Fig. 5. Experimental interferograms and phase profiles for lenses of increasing power.  
 (a) Interferogram and (d) unwrapped phase profile for  $V_{rms}(x,y)=5.65V$ ,  $V_{rms}(bias)=2.12V$ ,  $\phi=180^{\circ}$ .  
 (b) Interferogram and (e) unwrapped phase profile for  $V_{rms}(x,y)=5.65V$ ,  $V_{rms}(bias)=2.82V$ ,  $\phi=180^{\circ}$ .  
 (c) Interferogram and (f) unwrapped phase profile for  $V_{rms}(x,y)=4.60V$ ,  $V_{rms}(bias)=3.54V$ ,  $\phi=180^{\circ}$ .

Two dimensional (spherical) lenses can be produced by driving the opposing ends of the ‘ground’ electrode, which is oriented orthogonally to the ‘upper electrode’ as described above, with a second pair of driving voltages in a manner directly analogous to the case for the upper

electrode in the one dimensional case. This produces separate ‘x’ and ‘y’ voltage, and hence a spherical lens profile.

It is also possible to make other phase profiles using the techniques described. Tip and tilt can be produced trivially by controlling the relative amplitudes of the voltages applied to the opposing ends of the two electrodes, as described in refs [10, 11]. By using different driving frequencies for the two axes, they may be controlled independently, allowing the production of astigmatism oriented along the principle axes of the cell. Finally it is also possible to produce quasi-linear phase profiles and thus an axicon.

### 3. Results

Figure 5. shows interferograms and unwrapped  $x$ - and  $y$ - optical phase cross sections illustrating positive lens operation for different driving voltages. The phase shift in the driving voltage was  $\pi$ , and a second bias voltage was used to remove the effect of the LC threshold voltage. The voltages (shown in the figure captions) were applied to both electrodes to produce spherical lenses. In each case a positive lens profile is observed with a range of approximately (-3.2 to -13.5 waves of defocus) and (0.5 to 1 waves of astigmatism). The equivalent focal lengths were estimated using the equation,

$$f = \frac{d^2}{8\Delta nd},$$

where  $d$  is the lens diameter and  $\Delta nd$  is the optical path length difference across the length (the sag) calculated from the number of fringes degenerated. The approximate focal lengths in Fig. 5. varied from 6m to 1.5m. The total dynamic range for this type of addressing will be similar to other LC lens technology.

Figure 6 illustrates the effect on the optical phase profile of varying the phase shift ( $\phi$ ) between the voltages applied to the electrodes, without changing the amplitudes of either the driving or the bias voltages. The data were measured using a Zygo phase shifting interferometer.

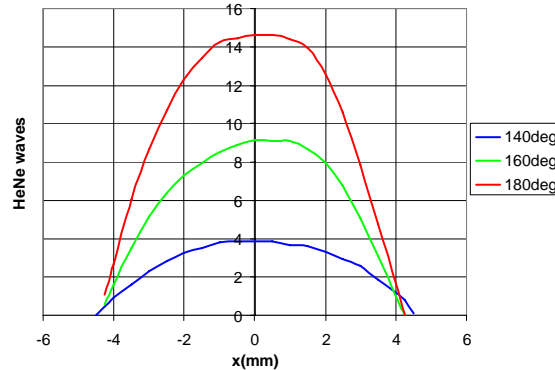


Fig. 6. Experimental phase profiles for values of  $\phi = 140^\circ$ ,  $160^\circ$  and  $180^\circ$   $V_{rms}(x,y)=4.5V$ ,  $V_{rms}(bias)=1.2V$  in each case.

It can be seen that as  $\phi$  is increased towards  $180^\circ$ , the total optical phase shift of the lens increases and the plateau in the optical profile becomes more pronounced, as indicated by the simulations shown in Fig. 2. The characteristic splayed ‘tails’ in the simulated phase profiles, visible at the periphery of the lens, are avoided by restricting the peripheral voltage to significantly less than the saturation voltage of the cell. The very pronounced plateau seen in Fig. 4 for the case of  $\phi=180^\circ$  is avoided by using a small bias voltage.

Figure 7 shows an interferogram and  $x$ - and  $y$ - optical phase cross sections, showing astigmatism and demonstrating both negative lens operation and independent control of the  $x$ - and  $y$ -axes

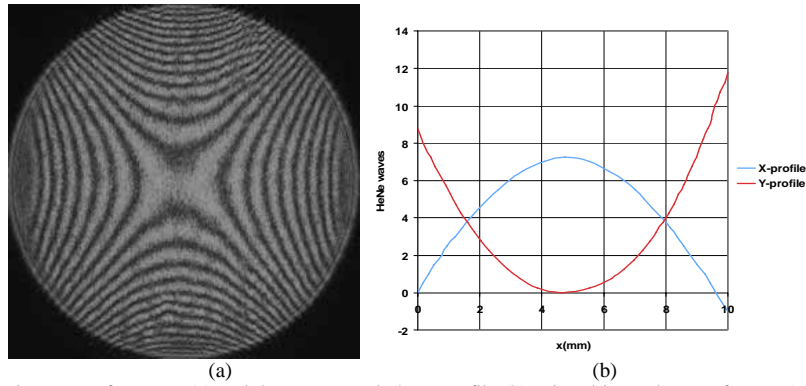


Fig. 7. Interferogram (a) and the unwrapped phase profile (b) using drive voltages of  $V_{xLF}=5.65$   $V_{rms}$ ,  $V_{xLF,bias}=2.12$   $V_{rms}$ ,  $\phi_x = \phi_y = 180^\circ$ ,  $V_{yLF}=6.7$   $V_{rms}$ ,  $V_{yHF}=2.35$   $V_{rms}$

Finally, in Fig. 8 we show a cross section of a lens configured to give a linear phase profile and therefore an (adaptive) axicon. This was achieved by setting  $\phi$  to  $180^\circ$ , and by choosing a bias and driving voltage pair which span the (quasi) linear operating range of the phase-voltage response of the LC cell. The results shown in Fig. 8 illustrate both the worst case (i.e. greatest deviation from linear) optical performance and greatest throw axicon which can be achieved with the cell used in the tests. Better optical performance can be achieved either by reducing the throw of the axicon or by using a thicker device.

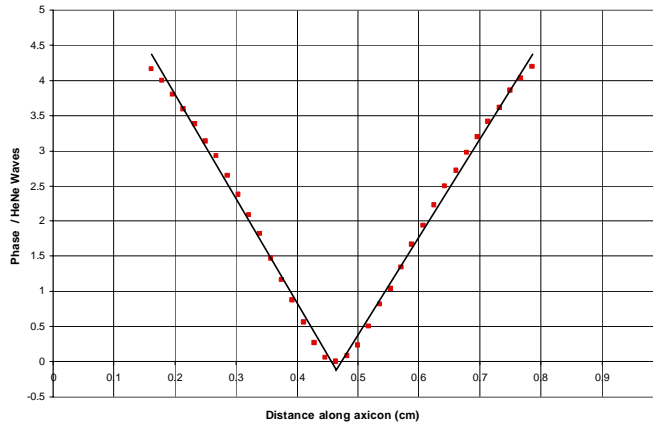


Fig. 8. Cross section of the phase profile of an axicon. The red data points are experiment data points measured using a Zygo phase shifting interferometer and black lines are least squares fits to each half of the data.

#### 4. Summary

We have demonstrated a novel method for addressing modal liquid crystal devices, overcoming some of the complexities of construction and limitations of performance of previously published modal LC lenses. We have demonstrated the production of positive and negative defocus and astigmatism aberration terms.

#### Acknowledgments

We would like to acknowledge the help and advice of Dr. Alexander Naumov, who first suggested this method of addressing LC devices. This work was partly funded by the EU and the EPSRC under the Eurocores SONS programme.